Free Radical Research, November 2009; 43(11): 1060–1071

informa
healthcare

Resveratrol protects against irradiation-induced hepatic and ileal damage via its anti-oxidative activity

AYLIZ VELIOĞLU-ÖĞÜNÇ[1], ÖZER ŞEHIRLI[2], HALE Z. TOKLU[2], HAZAN ÖZYURT[3], ALPASLAN MAYADAĞLI[3], EMEL EKŞIOĞLU-DEMIRALP[4], CAN ERZIK[5], ŞULE ÇETINEL[6], BERRAK Ç. YEĞEN[7], & GÖKSEL ŞENER[1]

[1]*Vocational School of Health Related Professions, Marmara University,* [2]*Department of Pharmacology, School of Pharmacy, Marmara University,* [3]*Radiation Oncology, Dr Lutfi Kirdar Kartal Research Hospital, Departments of* [4]*Hematology-Immunology,* [5]*Medical Biology,* [6]*Histology-Embryology, and* [7]*Physiology, School of Medicine, Marmara University, Istanbul, Turkey*

(Received 2 April 2009; revised 6 July 2009)

Abstract

The present study was undertaken to determine whether resveratrol (RVT) could ameliorate ionizing radiation-induced oxidative injury. After a 10-days pre-treatment with RVT (10 mg/kg/day p.o.), rats were exposed to whole-body IR (800 cGy) and the RVT treatment was continued for 10 more days after the irradiation. Irradiation caused a significant decrease in glutathione level, while malondialdehyde levels, myeloperoxidase activity and collagen content were increased in the liver and ileum tissues. Similarly, plasma lactate dehydrogenase and pro-inflammatory cytokine levels, 8-hydroxy-2′-deoxyguanosine and leukocyte apoptosis were elevated, while antioxidant-capacity was reduced in the irradiated rats as compared with the control group. Furthermore, Na^+, K^+-ATPase activity was inhibited and DNA fragmentation was increased in the ileal tissues. Resveratrol treatment reversed all these biochemical indices, as well as histopathological alterations induced by irradiation. In conclusion, supplementing cancer patients with adjuvant therapy of resveratrol may have some benefit for a more successful radiotherapy.

Keywords: *Irradiation, lipid peroxidation, glutathione, myeloperoxidase, resveratrol*

Introduction

Tissue injury from ionizing radiation ultimately begins with oxidative stress from radiolytic hydrolysis and formation of reactive oxygen species (ROS) [1]. It is believed that cytokine activity may be one of the major mechanisms playing a role in the long-term morbidity of the irradiation-induced oxidative tissue damage [2]. It has long been recognized that the most critical target of irradiation passing through living tissues is the DNA [3]. Additionally, lipids and proteins present in the structure of the cells are also attacked by free radicals induced by irradiation [4]. Radiation-induced damage may be repairable, but in some cases the repair is inaccurate [5,6], resulting in acute adverse health effects within hours to weeks or delayed effects within months to years after exposure. The adverse effects on the liver and intestines may result in severe complications, which may consequently cause the cessation of the radiation therapy [4,7]. Thus, these highly radiosensitive organs may frequently be considered as the dose limiting organs. Since radiation-induced cellular damage is attributed primarily to harmful effects of free radicals, molecules with direct free radical scavenging properties are particularly promising as radioprotectors. Among the best known radioprotectors, the sulphydryl compounds cysteine and cysteamine [8,9] have some serious side-effects and are considered to be toxic at

Correspondence: Göksel Sener, PhD, Marmara University, School of Pharmacy, Tıbbiye Cad. 34668 İstanbul, Turkey. Tel: 00 90 216 414 29 62. Fax: 00 90 216 345 29 52. Email: gsener@marmara.edu.tr

ISSN 1071-5762 print/ISSN 1029-2470 online
DOI: 10.1080/10715760903171100

the doses required for radioprotection. Similarly, amifostine, which was tolerated well in radiotherapeutic clinical trials, was reported to have some undesirable side-effects [10]. Thus, regarding the limited success of current biological modifiers targeting oxidative damage for radioprotection, there is absolutely a need for more potent and less toxic compounds, especially of herbal origin to boost antioxidant defense.

Resveratrol (3,5,4′-trans-trihydroxystilbene; RVT), a natural phytoalexin present in grapes, peanuts, mulberries and red wine, has various pharmacological effects, including anti-inflammatory properties, modulation of lipid metabolism and prevention of cancer [11–14]. Its anti-inflammatory effect is related to inhibiting oxidation, leukocyte priming and expression of inflammatory mediators. Recently, it has been found to prevent and improve cardiovascular or microcirculatory disorders by protecting the vascular endothelium, modulation of lipid metabolism, increasing cellular nitric oxide levels, as well as inhibiting platelet aggregation [11–13,15]. Similarly, Gresele et al. [16] demonstrated that resveratrol activates eNOS, blunts the pro-inflammatory pathway and inhibits ROS production. On the other hand, RVT modulates the NO/NOS system, by increasing iNOS and eNOS expression, NOS activity and NO production [17].

Based on the aforementioned studies, using biochemical and histopathological approaches, the present study was aimed to examine the antioxidant and radioprotective abilities of RVT against irradiation-induced damage of the dose limiting organs, namely liver and intestines.

Materials and methods

Experimental design

All experimental protocols were approved by the Marmara University Animal Care and Use Committee. Male Sprague Dawley rats (200–250 g, 3 months old) were obtained from Marmara University Animal House and were kept at a constant temperature ($22 \pm 1^{\circ}C$) with 12-h light and dark cycles. All chemicals used in the study were purchased from Sigma Chemical Co. (St. Louis, MO).

A group of rats received a 10-day pretreatment with either 10 mg/kg/day RVT (99% purity; Mikrogen Pharmaceuticals, Turkey; $n = 8$) or vehicle (0.5% carboxymethyl cellulose, CMC; $n = 8$) by orogastric gavage before they were exposed to irradiation and the treatments were continued for the following 10 days after the irradiation. The rationale in choosing the RVT dose is based on our previous studies [18,19]. Rats received a single whole-body X-ray irradiation (IR) of 800 cGy under ketamine anaesthesia (100 mg/kg intraperitoneally) with a linear accelerator (Linac, Saturn 41, General Electric, France) producing 6 MV photons at a focus. Animals were returned to their home cages following irradiation. Another set of rats that served as the control groups were treated with either vehicle ($n = 8$) or RVT ($n = 8$) in a similar manner as the irradiated groups, but did not have irradiation. On the 11^{th} day of irradiation, the rats were decapitated and trunk blood was obtained for the measurement of pro-inflammatory cytokines and for the evaluation of oxidant–antioxidant status, leukocyte apoptosis and hepatic functions. Ileum and liver samples were obtained for the determination of tissue malondialdehyde and glutathione levels, myeloperoxidase activity and collagen contents. Formation of reactive oxygen species in both tissue samples was monitored by using chemiluminescence (CL) technique. In the ileal tissues, DNA fragmentation was analysed as an indicator of mucosal apoptosis, while Na^+-K^+ ATPase activity was measured to evaluate membrane transport function indirectly. Both the ileal and hepatic tissues were also examined microscopically.

Blood assays

The hepatic function tests, aspartate aminotransferase (AST) and alanine aminotransferase (ALT) [20], as well as lactate dehydrogenase (LDH), an indicator of tissue damage [21], were determined spectrophotometrically using an automated analyser (Bayer Opera biochemical analyzer, Germany). Using enzyme-linked immunosorbent assay (ELISA) kits specific for rat cytokines, plasma levels of tumour necrosis factor-alpha (TNF-α), interleukin-1 beta (IL-1β) and IL-6 were quantified according to the manufacturer's instructions and guidelines (Biosource Europe S.A., Nivelles, Belgium). The total antioxidant capacity (AOC) in plasma was measured by a colourimetric test system (ImAnOx, cataloge no.KC5200, Immunodiagnostic AG, D-64625 Bensheim) according to the instructions provided by the manufacturer. Plasma 8-hydroxy-2′-deoxyguanosine (8-OHdG) content was determined by ELISA method (Highly Sensitive 8-OHdG ELISA kit, Japan Institute for the Control of Aging, Shizuoka, Japan) in the extracted DNA solution. These particular assay kits were selected because of their high degree of sensitivity, specificity, inter- and intra-assay precision and small amount of plasma sample required to conduct the assay.

Evaluation of apoptosis and cell death in leukocytes

Apoptosis was induced by using phorbol myristate acetate (PMA, Sigma-Aldrich, Taufkirchen, Germany) as previously described with some modifications [22]. Briefly, erythrocytes from heparinized blood samples of the groups were discarded using erythrocyte lysis solution. White blood cells were washed and re-suspended in phosphate buffer

solution (PBS). For each apoptosis experiment, 1×10^5 cells/ml were distributed into two tubes. One tube was induced for apoptosis using 100 ng/ml of PMA at 37°C for 2 h, while the other was incubated at the same temperature without stimulation (control). To demonstrate early apoptosis, cells were washed with PBS following stimulation and were labelled with annexin V (Biovision, Mountain view, CA) according to manufacturer's instructions. Briefly, 1 µl of annexin V was added to the tubes and cells were incubated in the dark for 15 min. Once propidium iodide (20 ng/ml, Sigma-Aldrich, Taufkirchen, Germany) was added to label late apoptosis and cell death, 10 000 cells were immediately acquired by flow cytometry (FACS CANTO, Becton Dickinson, Mountain View, CA). For analysis, lymphocytes and neutrophils were separately gated according to their granularity and size on forward scatter (FSC) vs Side Scatter (SSC) plot by using Diva software (Becton Dickinson, Mountain View, CA). Early apoptosis, late apoptosis, necrosis and cell death were evaluated on Fluorescence 1 (FL1 for Annexin V) vs Fluorescence 3 (FL3 for propidium iodide) plots. The percentage of cells stained with only Annexin V was evaluated as early apoptosis, while the percentage of cells stained with both Annexin V and propidium iodide was evaluated as late apoptosis and the percentage of cells stained only with propidium iodide was evaluated as cell death and/or necrosis. Comparisons between the groups were performed by using ratios of apoptosis and cell death. Ratios of apoptosis and cell death were calculated by dividing the percentage values of after-stimulation to those of prior to stimulation for each individual sample.

Tissue chemiluminescence (CL) assay

Measurements were made at room temperature using a Junior LB 9509 luminometer (EG&G Berthold, Germany). Specimens (~0.1 g) were put into vials containing PBS and 4-(2-Hydroxyethyl) piperazine-1-ethanesulphonic acid (HEPES) buffer (0.5 M PBS containing 20 mM HEPES, pH 7.2). ROS were quantitated after the addition of either lucigenin or luminol for a final concentration of 0.2 mM. Luminol detects a group of reactive species, i.e. hydroxyl radicals ($OH^{\bullet}$), hydrogen peroxide (H_2O_2), hypochlorous acid (HOCl), while lucigenin is selective for superoxide radicals ($O_2^{\bullet -}$) [23,24]. Counts were obtained at 1 min intervals and the results were given as the area under curve (AUC) for a counting period of 5 min. Counts were corrected for wet tissue weight (rlu/mg tissue) [25].

Tissue malondialdehyde and glutathione assays

Tissue samples (0.3–0.5 g) were homogenized with ice-cold 150 mM KCl (w/v, 10%) for the determination of malondialdehyde (MDA) and glutathione (GSH) levels using the homogenizer (Janke & Kunkel IKA-Labortechnik Ultra-Turrax T25). Lipid peroxidation was expressed in terms of MDA equivalents using an extinction coefficient of 1.56×10^5 M^{-1} cm^{-1} and results were expressed as nmol MDA/g tissue [26]. GSH measurements were performed using a modification of the Ellman procedure [27]. Briefly, after centrifugation at 2000 g for 10 min, 0.5 ml of supernatant was added to 2 ml of 0.3 mol/l $Na_2HPO_4.2H_2O$ solution. A 0.2 ml solution of dithiobisnitrobenzoate (0.4 mg/ml 1% sodium citrate) was added and the absorbance at 412 nm was measured immediately after mixing. GSH levels were calculated using an extinction coefficient of 1.36×10^4 M^{-1} cm^{-1}. Results were expressed in µmol GSH/g tissue.

Measurement of tissue myeloperoxidase activity

Tissue MPO activity was measured in a procedure similar to that documented by Hillegass et al. [28]. Tissue samples (0.3–0.5 g) were homogenized (w/v 10%) in 50 mM potassium phosphate buffer (PB, pH 6.0) and centrifuged at 41 400 g (10 min); pellets were suspended in 50 mM PB containing 0.5% hexadecyltrimethylammonium bromide (HETAB). After three freeze and thaw cycles, with sonication between cycles, the samples were centrifuged at 41 400 g for 10 min. Aliquots (0.3 ml) were added to 2.3 ml of reaction mixture containing 50 mM PB, o-dianisidine and 20 mM H_2O_2 solution. One unit of enzyme activity was defined as the amount of MPO present that caused a change in absorbance measured at 460 nm for 3 min. MPO activity was expressed as U/g tissue.

Histopathological analysis and tissue collagen measurement

Tissue samples were fixed in 10% (v/v) buffered p-formaldehyde and prepared for routine paraffin embedding. Tissue sections (6 µm) were then stained with Hematoxylin and Eosin and examined under a light microscope (Olympus-BH-2) by an experienced histologist, who was unaware of the treatment conditions.

Extra tissue samples that were fixed in p-formaldehyde and embedded in paraffin were cut (15 µm) and used for tissue collagen measurement as a free radical-induced fibrosis marker. Evaluation of collagen content was made according to the method published by Lopez de Leon and Rojkind [29], based on selective binding of the dyes Sirius Red and Fast Green FCF to collagen and non-collagenous components, respectively. Both dyes were eluted readily and simultaneously by using 0.1 N NaOH-methanol (1:1, v/v). Finally, the absorbances at 540 and 605 nm were used to determine the amount of collagen and protein, respectively.

Tissue DNA fragmentation assay

Mucosal samples (0.10–0.15 mg) from ileum were homogenized in 10 volumes of a lysis buffer (5 mM Tris HCL, 20 mM ethylene diamine tetraacetic acid [EDTA], 0.5% (v/v) *t*-octylphenoxypolyethoxyethanol [Triton-X 100]; pH = 8.0). Two separate samples of 1 mL were taken from the mucosal samples and centrifuged at 25 000 g for 30 min to separate the intact chromatin in the pellet from the fragmented DNA in the supernatant [30]. The pellet was re-suspended in 1 mL of Tri-EDTA buffer (pH = 8.0), 10 mM:1 mM, respectively. Both the supernatant and the re-suspended pellet were assayed for the DNA content by diphenylamine reaction described by Burton [31]. Tricarboxylic acid (TCA, 25%) was added to both tubes containing the re-suspended pellet and supernatant and the tubes were kept at 4°C overnight. The samples were centrifuged then at 4°C and 25 000 g for 30 min. The supernatants were discarded and 5% freshly prepared TCA was added to the pellets in both tubes. The tubes were shaken for 20 min at 95°C and freshly prepared diphenylamine (DPA) solution (15 mg DPA dissolved in 1 mL glacial acetic acid with the addition of 1 μL concentrated sulphuric acid) was added in a volume twice the samples. After the samples were left at 37°C for 4 h, optical densities were read then at 595 nm.

Measurement of tissue Na^+, K^+-ATPase activity

Measurement of Na^+, K^+-ATPase activity is based on the measurement of inorganic phosphate released by ATP hydrolysis during the incubation of homogenates with an appropriate medium containing 3 mM ATP as a substrate. The total ATPase activity was determined in the presence of 100 mM NaCl, 5 mM KCl, 6 mM $MgCl_2$, 0.1 mM EDTA, 30 mM Tris–HCl (pH 7.4), while the Mg^{2+}-ATPase activity was determined in the presence of 1 mM ouabain. The difference between the total and the Mg^{2+}-ATPase activities was taken as a measure of the Na^+, K^+-ATPase activity [32]. Tissue samples (0.3–0.5 g) were homogenized in 0.32 M sucrose (w/v: 10%). The reaction was initiated with the addition of the homogenate sample and after a 5-min pre-incubation period at 37°C Na_2ATP was added. Following a 10-min re-incubation, the reaction was terminated by the addition of ice-cold 6% perchloric acid. The mixture was then centrifuged at 3500 g and Pi in the supernatant fraction was determined by the method of Fiske and Subbarow [33]. The specific activity of the enzyme was expressed as nmol Pi mg^{-1} protein h^{-1}. The protein concentration of the supernatant was measured by the Lowry et al. [34] method.

Statistics

Statistical analysis was carried out using GraphPad Prism 3.0 (GraphPad Software, San Diego, CA). All data were expressed as means ± SEM. Groups of data were compared with an analysis of variance (ANOVA) followed by Tukey's multiple comparison tests. Values of $p < 0.05$ were regarded as significant.

Results

Plasma AST/ALT levels and LDH activity, used as indices of hepatic injury and of generalized tissues damage, were increased significantly in irradiated animals ($p < 0.001$), while RVT administration prevented these elevations ($p < 0.001$; Table I).In the vehicle-treated IR groups, TNF-α, IL-1β and IL-6 levels were significantly increased ($p < 0.001$) when compared to control groups treated with either vehicle or RVT, while this IR-induced rise in plasma pro-inflammatory cytokines was reduced ($p < 0.05$–0.001) when the rats received RVT treatment before and after irradiation (Table I). Similarly, oxidative DNA marker 8-OHdG was increased in the plasma of vehicle-treated irradiation groups, while total antioxidant capacity (AOC) was depressed significantly ($p < 0.001$). On the other hand, RVT treatment in

Table I. Plasma alanine aminotransferase (ALT) and aspartate aminotransferase (AST), lactate dehydrogenase (LDH) activity, TNF-α, IL-1β, IL-6, total antioxidant capacity (AOC; pg/ml) and 8-hydroxy-2′-deoxyguanosine (8-OHdG) levels of the vehicle or resveratrol (RVT) treated control and irradiated groups. For each group, $n = 8$.

	Control		Irradiation	
	Vehicle-treated	RVT-treated	Vehicle-treated	RVT-treated
AST (U/l)	27.2 ± 3.7	30.2 ± 2.9	103.2 ± 9.9***	51.2 ± 5.2^{+++}
ALT (U/l)	33.3 ± 2.8	34.3 ± 1.8	63.0 ± 4.5***	36.7 ± 3.3^{+++}
LDH (U/l)	1495 ± 119	1396 ± 208	4703 ± 341***	2539 ± 301*,$^{+++}$
TNF-α (pg/ml)	7.4 ± 1.3	7.9 ± 1.1	36.2 ± 4.1***	14.0 ± 2.3^{+++}
IL-1β (pg/ml)	6.0 ± 0.5	5.3 ± 0.7	44.9 ± 6.6***	29.3 ± 2***,$^{+}$
IL-6 (pg/ml)	2.8 ± 0.3	3.3 ± 0.3	41 ± 5***	15 ± 1.5*,$^{+++}$
AOC (pg/ml	334 ± 11	349 ± 15	43 ± 4***	194 ± 22***,$^{+++}$
8-OHdG (ng/ml)	0.33 ± 0.03	0.34 ± 0.03	5.84 ± 0.4***	3.7 ± 0.1***,$^{+++}$

*$p < 0.05$, ***$p < 0.001$; compared to control group; $^{+}p < 0.05$, $^{+++}p < 0.001$ compared to untreated IR group. Data are given as mean ± SEM and each group consists of eight rats.

irradiated rats reduced the plasma 8-OHdG level and prevented the reduction in AOC ($p < 0.001$, Table I).

Annexin V stainings alone were evaluated as early apoptosis, while annexin V along with propidium iodide stainings were evaluated as late apoptosis. Both early and late apoptosis ratios in neutrophils were significantly higher in the vehicle-treated irradiation groups when compared to control groups ($p < 0.05$–0.001, Figure 1A and B). In addition, irradiation has significantly induced neutrophil death ($p < 0.001$; Figure 1C). Similar results were obtained for the early and late apoptosis and cell death ratios of lymphocytes from vehicle-treated rats that had irradiation ($p < 0.01$–0.001, Figure 2A–C). On the other hand, RVT administration abolished the apoptotic effect of irradiation on both neutrophils and lymphocytes and prevented the cell death ratio in both types of leukocytes ($p < 0.001$, Figures 1 and 2).

Luminol and lucigenin chemiluminescence (CL) values of both hepatic and ileal tissues were found to

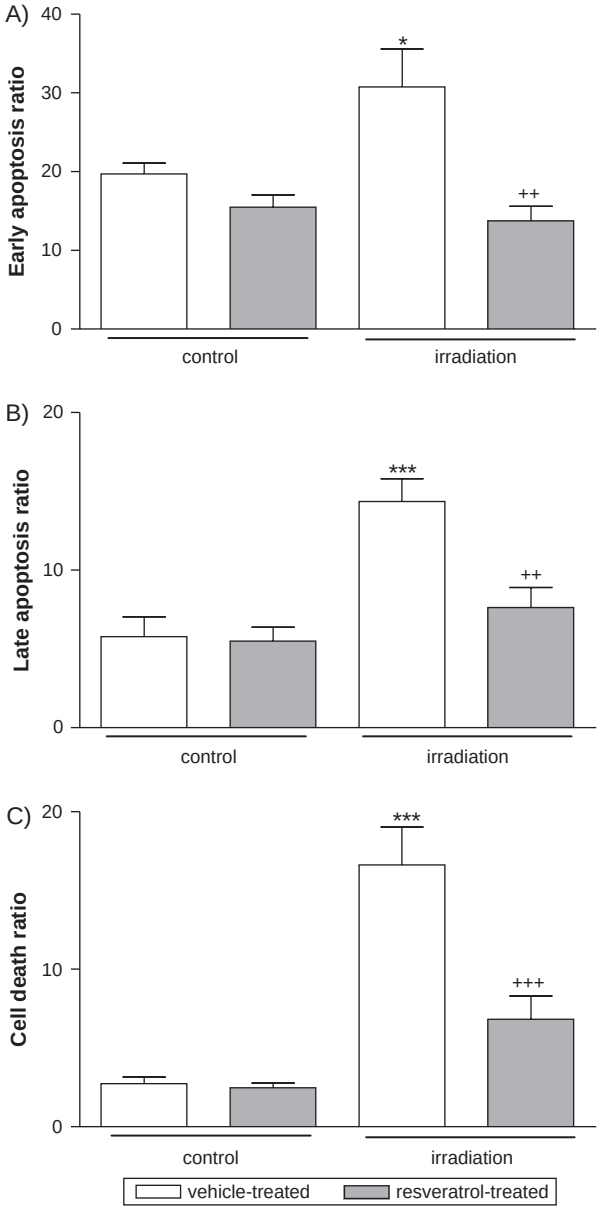

Figure 1. (A) Early apoptosis, (B) late apoptosis and (C) cell death of neutrophils obtained from vehicle- or resveratrol-treated rats induced with irradiation. Early and late apoptosis and cell death ratios were calculated by dividing the values of after-stimulation to the values obtained without phorbol myristate acetate stimulation. $^{*}p < 0.05$ and $^{***}p < 0.001$ compared with vehicle-treated control group; $^{++}p < 0.01$, $^{+++}p < 0.001$ compared with vehicle-treated irradiation group. Data are given as mean ± SEM and each group consists of eight rats.

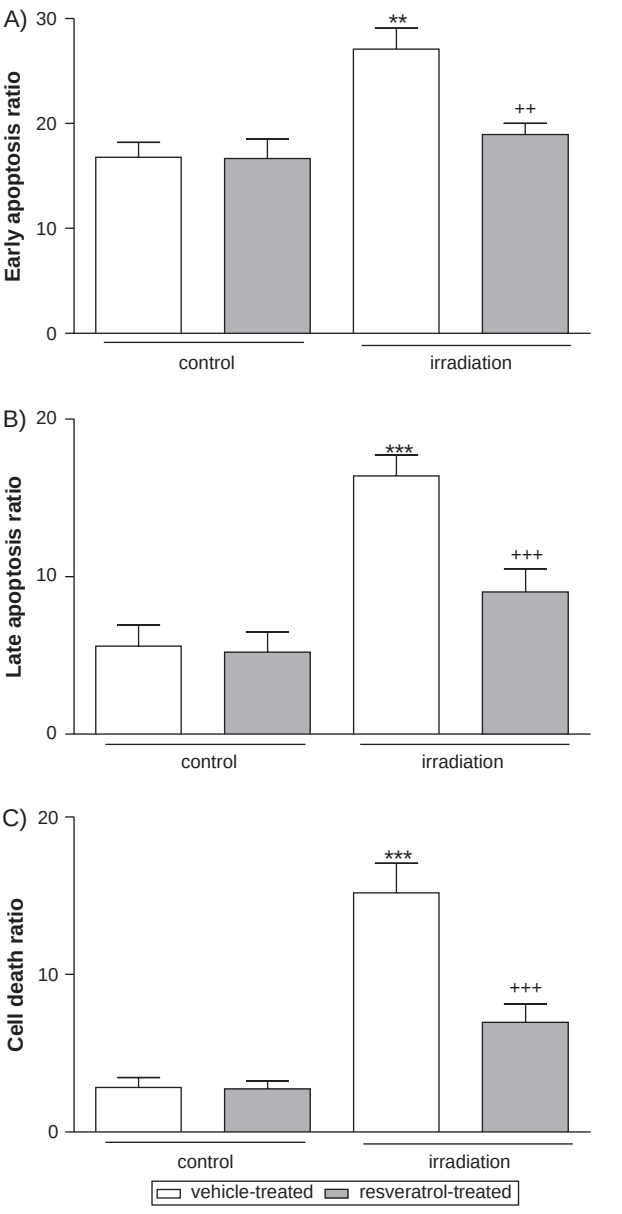

Figure 2. (A) Early apoptosis, (B) late apoptosis and (C) cell death of lymphocytes obtained from vehicle- or resveratrol-treated rats induced with irradiation. Early and late apoptosis and cell death ratios were calculated by dividing the values of after-stimulation to the values obtained without phorbol myristate acetate stimulation. $^{**}p < 0.01$ and $^{***}p < 0.001$ compared with vehicle-treated control group; $^{++}p < 0.01$, $^{+++}p < 0.001$ compared with vehicle-treated irradiation group. Data are given as mean ± SEM and each group consists of eight rats.

be significantly higher in the irradiated and vehicle-treated groups than those in the control groups ($p < 0.05$; $p < 0.001$). RVT treatment, however, given prior to and after irradiation, completely suppressed ROS generation in these tissues, as detected by both probes ($p < 0.05$; $p < 0.001$; Figure 3).

As compared to those of the control groups, MDA levels in the hepatic and ileal tissues were significantly higher in the irradiated group that has received vehicle treatment ($p < 0.001$, Figure 4), while treatment with RVT significantly ($p < 0.001$) prevented the lipid peroxidation in both tissues. In accordance with these, GSH levels in the studied tissues of vehicle-treated rats were depressed significantly following irradiation ($p < 0.01$–0.001; Figure 5) and RVT treatment prevented the depletion of GSH in both tissues ($p < 0.05$). Similarly, MPO activity was significantly increased in the liver and ileum of vehicle-treated irradiated groups ($p < 0.001$), indicating increased tissue neutrophil infiltration [16], while RVT treatment decreased, but not completely prevented irradiation-induced neutrophil infiltration in these tissues ($p < 0.001$, Figure 6).

Collagen contents in the hepatic and ileal tissues of vehicle-treated and irradiated group were markedly increased as compared to control group, implying enhanced tissue fibrotic activity due to irradiation ($p < 0.05$–0.001, Figure 7). On the other hand, in the rats that have received RVT treatment, tissue collagen levels were not different than those of the non-irradiated control rats.

The activity of Na^+-K^+ ATPase in the ileum of the irradiated rats that received vehicle treatment was significantly lower than that of the non-irradiated control groups ($p < 0.001$). However, when the treatment regimen was replaced with RVT, irradiation-induced reduction in ileal Na^+-K^+ ATPase activity was abolished ($p < 0.05$; Figure 8A). Concomitant with that, DNA fragmentation was elevated in the ileal mucosae of irradiated rats with vehicle treatment ($p < 0.001$, Figure 8B), however RVT treatment prevented the DNA damage induced by irradiation ($p < 0.001$).

The histopathological analysis in liver tissues of the control groups showed regular morphology (Figure 9A), while in the liver of vehicle-treated irradiation group, sinusoidal dilatations and degeneration of hepatocytes were observed and the density of Kupffer cells was increased (Figure 9B). On the other hand, in the RVT-treated and irradiated group, the sinusoids were regenerated and the hepatocytes demonstrated a nearly regular morphology (Figure 9C).

Ileal tissues of the control groups showed a regular morphology (Figure 10A) with intact epithelial and glandular structures. In the irradiated group that has received vehicle treatment, enlargement of goblet cells, epithelial detachments and accumulation of leukocytes were prominent (Figure 10B). However, in the RVT-treated and irradiated group, the morphology was nearly the same as the control group, with a normal epithelial and glandular appearance (Figure 10C).

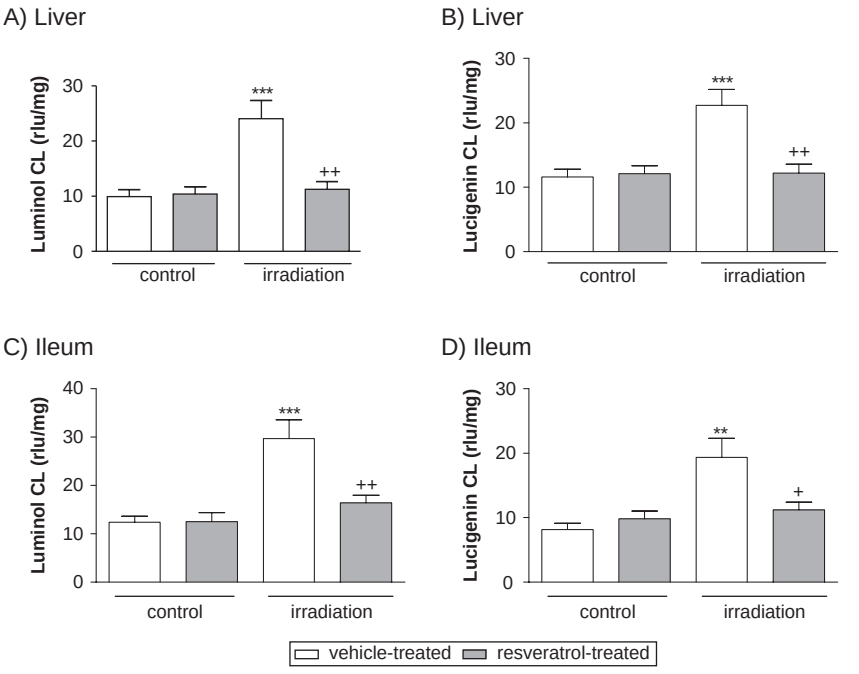

Figure 3. Luminol chemiluminescence (CL) in the (A) liver and (C) ileum tissues and lucigenin CL in the (B) liver and (D) ileum tissues of vehicle or resveratrol-treated rats induced with irradiation. Groups of data were compared with an analysis of variance (ANOVA) followed by Tukey's multiple comparison tests. $^{**}p < 0.01$ and $^{***}p < 0.001$ compared with vehicle-treated control group; $^{+}p < 0.05$, $^{+++}p < 0.001$ compared with vehicle-treated irradiation group. Data are given as mean ± SEM and each group consists of eight rats.

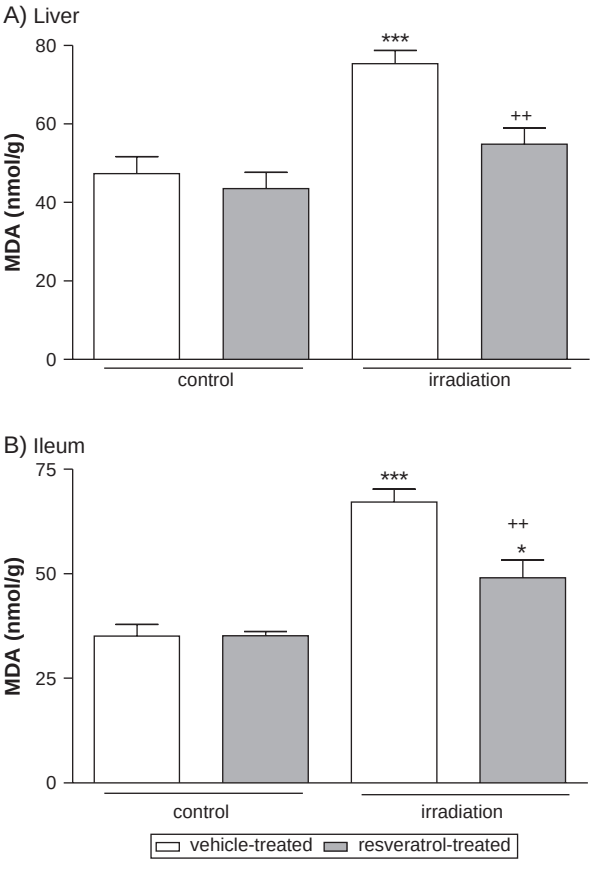

Figure 4. Malondialdehyde (MDA) levels in the (A) liver and (B) ileum tissues of vehicle or resveratrol-treated rats induced with irradiation. Groups of data were compared with an analysis of variance (ANOVA) followed by Tukey's multiple comparison tests. $^{*}p<0.05$ and $^{***}p<0.001$ compared with vehicle-treated control group; $^{++}p<0.01$ compared with vehicle-treated irradiation group. Data are given as mean ± SEM and each group consists of eight rats.

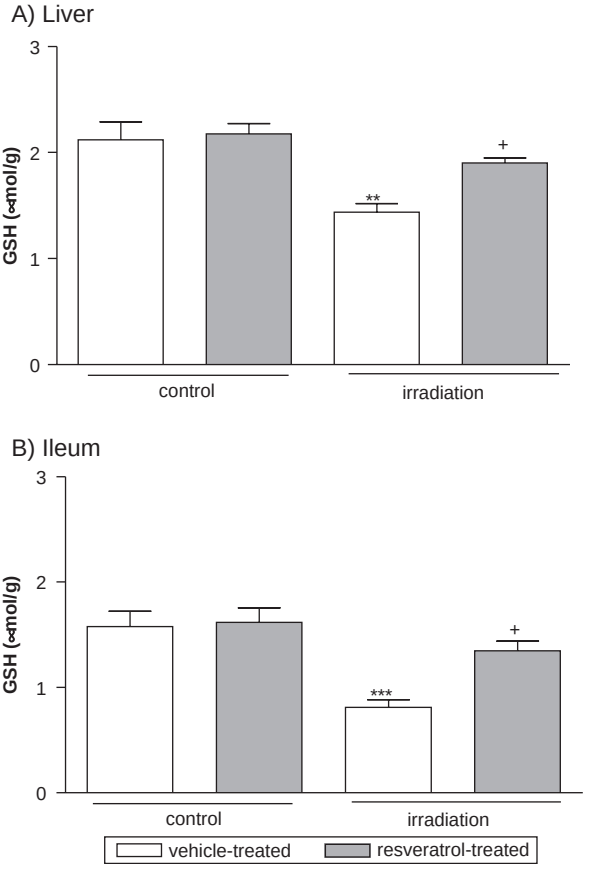

Figure 5. Glutathione (GSH) levels in the (A) liver and (B) ileum tissues of vehicle or resveratrol-treated rats induced with irradiation. Groups of data were compared with an analysis of variance (ANOVA) followed by Tukey's multiple comparison tests. $^{**}p<0.01$ and $^{***}p<0.001$ compared with vehicle-treated control group; $^{+}p<0.05$ compared with vehicle-treated irradiation group. Data are given as mean ± SEM and each group consists of eight rats.

Discussion

Radiation therapy is a common and effective tool in the management of a wide variety of tumours and in some cases it may be the single best treatment of cancer. However, the radiosensitivity of normal tissues adjacent to the tumour, which are unavoidably exposed to radiation, limits therapeutic gain. The present results demonstrate that whole-body irradiation causes oxidative tissue damage in the liver and ileum of the rats, as assessed by increased lipid peroxidation and neutrophil infiltration, enhanced fibrosis and decreased GSH levels. Treatment with RVT, by depressing lipid peroxidation, neutrophil infiltration and replenishing GSH content in these tissues, demonstrated a protective effect against oxidative injury due to irradiation. Furthermore, RVT treatment attenuated irradiation-induced impairment in liver functions and decreased irradiation-induced elevations in plasma cytokines, LDH activity and oxidative damage of DNA.

Irradiating biological material leads to a rapid burst of ROS, generated primarily because of the ionizing of water molecules [35], which then interact with biological target molecules, causing lipid peroxidation and DNA damage and subsequently resulting in cell killing and mutations [36]. In the present study, MDA, a marker of lipid peroxidation, was increased in the liver and ileum of whole-body irradiated rats, indicating the presence of radiation-induced oxidative damage. Moreover, current CL data support that tissue injury induced by irradiation involves the generation of toxic oxygen metabolites. On the other hand, RVT treatment with its antioxidant activity prevented elevations in tissue MDA and attenuated the increases in tissue luminol- and lucigenin-enhanced CL levels, suggesting that RVT ameliorates radiation-induced oxidative injury, in part, by scavenging reactive oxygen radicals. In accordance with the present findings, an *in vitro* study has recently shown that the protective effects of RVT on UV-irradiated skin cells involve a reduction in ROS production [37].

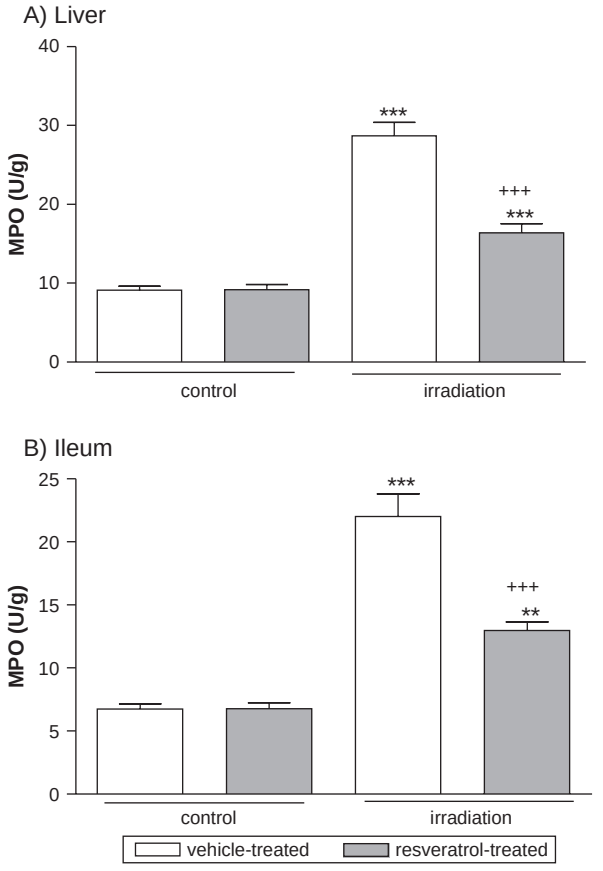

Figure 6. Myeloperoxidase (MPO) activity in the (A) liver and (B) ileum tissues of vehicle or resveratrol-treated rats induced with irradiation. Groups of data were compared with an analysis of variance (ANOVA) followed by Tukey's multiple comparison tests. $^{**}p<0.01$ and $^{***}p<0.001$ compared with vehicle-treated control group; $^{+++}p<0.001$ compared with vehicle-treated irradiation group. Data are given as mean ± SEM and each group consists of eight rats.

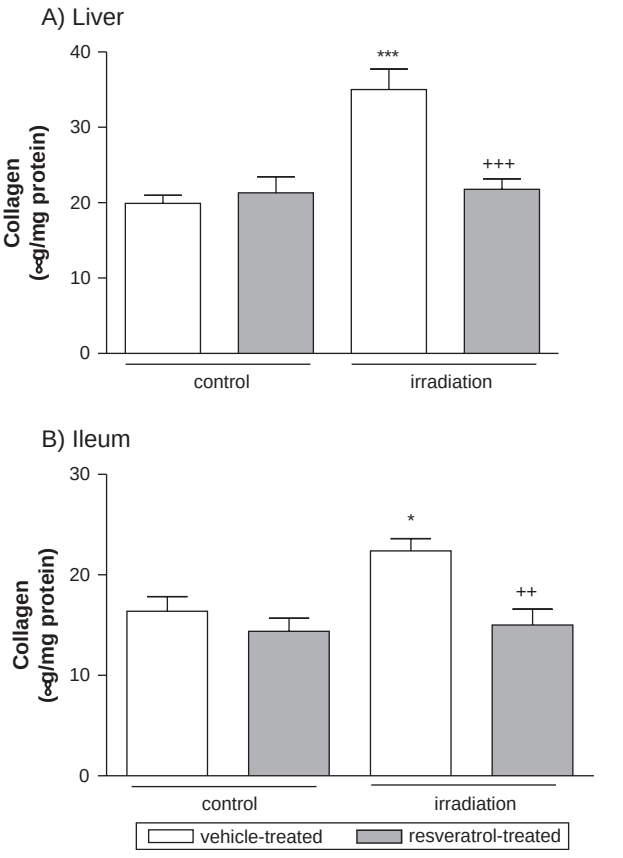

Figure 7. Collagen contents in the (A) liver and (B) ileum tissues of vehicle or resveratrol-treated rats induced with irradiation. Groups of data were compared with an analysis of variance (ANOVA) followed by Tukey's multiple comparison tests. $^{*}p<0.05$ and $^{***}p<0.001$ compared with vehicle-treated control group; $^{++}p<0.01$ and $^{+++}p<0.001$ compared with vehicle-treated irradiation group. Data are given as mean ± SEM and each group consists of eight rats.

Cell's ability to counteract ROS over-production depends on the capacity of the endogenous antioxidant defenses, whereas radiation exposure alters the balance of these defense systems [38]. It has been demonstrated that irradiation causes significant increases in MDA levels along with significant decreases in the antioxidant enzyme activities, such as superoxide dismutase (SOD) and catalase (CAT) and glutathione peroxidase (GSH-Px) [39,40]. In the current study, RVT treatment preserved the hepatic and ileal GSH stores that were depleted in the non-treated irradiated group, suggesting the antioxidant and free-radical scavenging effects of RVT. In accordance with the present results, it was shown that RVT maintains the levels of glutathione during oxidative stress and stimulates the enzymes involved in glutathione synthesis [11,41]. Furthermore, it was shown that RVT provided cardioprotection by preventing the reduction in GSH/GSSH ratio in ischemic cardiomyocytes, suggesting the role of RVT in the regulation of intracellular redox environment [42]. Similarly, decreases in SOD and CAT activities induced by other oxidants, such as doxorubicin or lipopolysaccharide, were also reversed with RVT treatment [43,44].

Both clinical and experimental studies have shown that irradiation is perceived by tissue macrophages and monocytes, which in turn secrete IL-1, TNF-α [2,45,46] and thereby perpetuate the inflammatory and fibrogenic processes of radiation damage [2]. Activated neutrophils can induce or exacerbate tissue injury through the production of oxygen metabolites [47] by activating cytotoxic enzymes such as elastase, proteases, lactoferrin and MPO [48]. As evidenced in the present study, ionizing radiation resulted in increased serum TNF-α, IL-1β and IL-6 levels, indicating the role of these pro-inflammatory cytokines in radiotherapy-induced toxicity. Accordingly, the presence of increased neutrophil accumulation, as assessed by elevated MPO activity in the liver and ileum, indicates that radiation-induced oxidative injury in these tissues involves the contribution of neutrophil accumulation. Moreover, the current findings show that irradiation-induced toxicity is

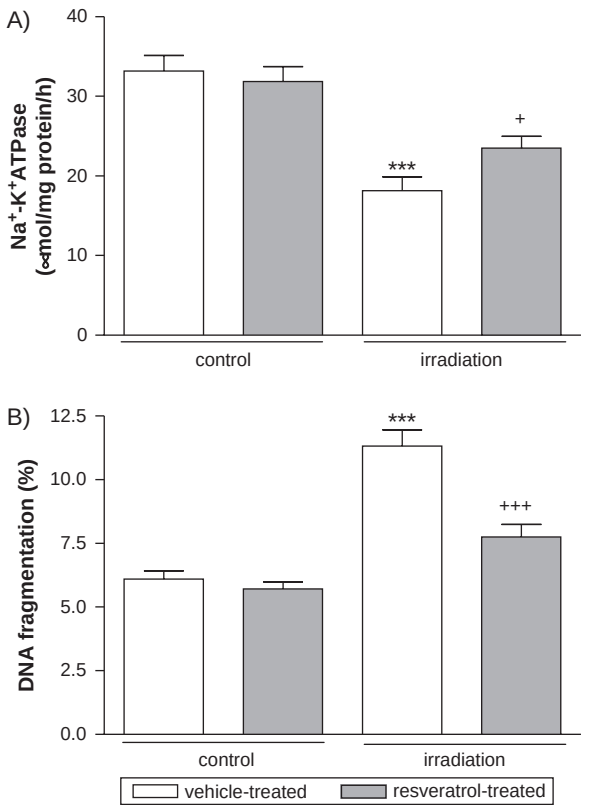

Figure 8. (A) Na^+-K^+ ATPase activity and (B) DNA fragmentation (%) in the ileum tissues of of vehicle or resveratrol-treated rats induced with irradiation. Groups of data were compared with an analysis of variance (ANOVA) followed by Tukey's multiple comparison tests. ***$p<0.001$ compared with vehicle-treated control group; $^{+}p<0.05$ and $^{+++}p<0.001$ compared with vehicle-treated irradiation group. Data are given as mean±SEM and each group consists of eight rats.

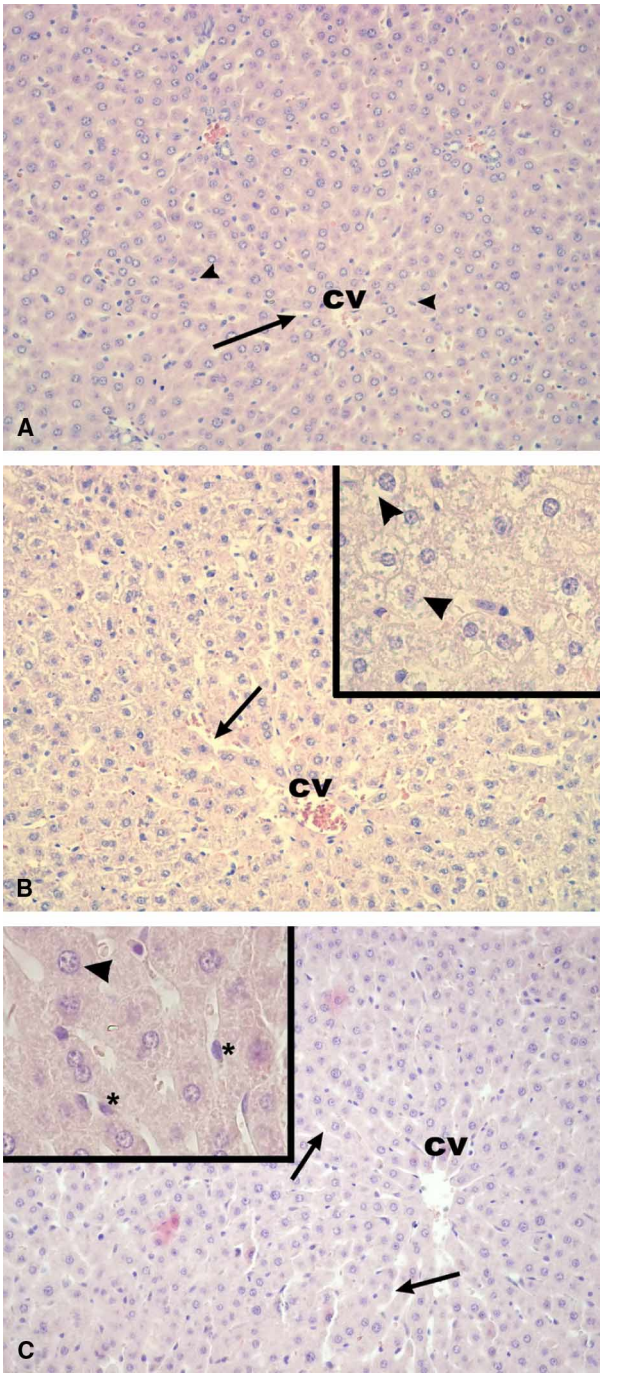

Figure 9. (A) Control liver with sinusoids (arrow) and hepatocytes, Kuppfer cells (arrowheads), central vein (cv); (B) Radiated liver, moderate dilation of sinusoids (arrow), the devastating degeneration of hepatocytes (arrowheads); (C) resveratrol treated liver,showing the regenerated morphology with restored sinusoids (arrows) and hepatocytes (arrowheads) and Kupffer cells (*). (original magnifications, ×200 and insets ×400).

associated with enhanced apoptosis of leukocytes and gut mucosal cells. On the other hand, RVT depressed the plasma levels of cytokines, effectively inhibited apoptosis and prevented neutrophil recruitment, suggesting that the protective effect of RVT against radiation-induced oxidative injury of the liver and ileum may involve its inhibitory effect on tissue neutrophil infiltration and neutrophil-derived cytokine response.

It has been suggested that LDH activity was abnormally increased and Na^+, K^+-ATPase activity was greatly inhibited when tissues and organs were injured [49]. More specifically, Keelan et al. [50] have shown that external abdominal irradiation-induced alterations in intestinal morphology and function were associated with reduced intestinal Na^+, K^+-ATPase activity. Similarly, Lebrun et al. [51] have also reported that following 8 Gy γ-radiation, which led to malabsorptive diarrhoea in rats, Na^+, K^+-ATPase activity in small intestinal mucosa was decreased. The results of our study are in agreement with these observations, since plasma LDH level was significantly increased as an indicative of generalized tissue injury and ileal Na^+, K^+-ATPase activity was decreased due to oxidative membrane damage. On the other hand, RVT treatment reversed these changes and improved the histological appearances, indicating its protective effects against irradiation-induced oxidative stress.

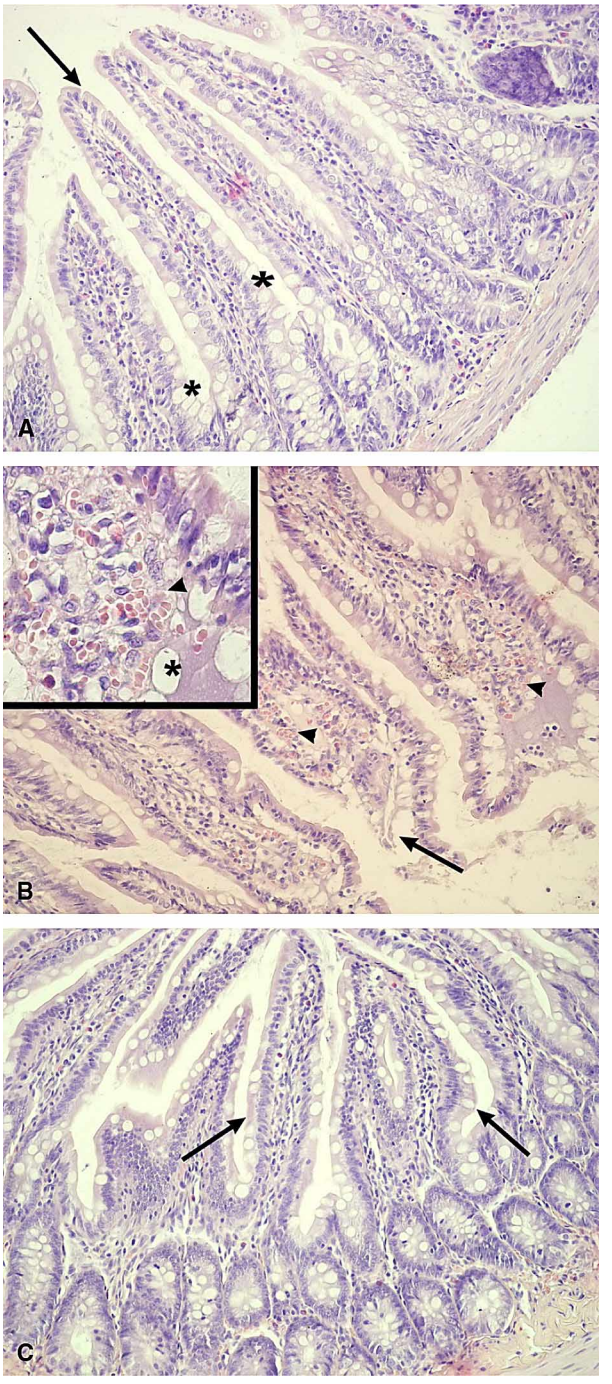

Figure 10. (A) Control group, well designed epithelium (arrow) and goblet cells (*), (B) Radiated group, detachment of epithelium and congestion in the lamina propria (arrowheads), degenerated glands (arrow) and enlarged goblet cells (*) were observed; (C) Resveratrol-treated group, the epithelial layout was regenerated (arrows) and there appeared minimal congestion. (Original magnifications, ×200 and insets ×400.)

In vital organs, irradiation-induced oxidative injury can result in the development of progressive fibrosis and organ failure [52], a major factor in limiting the radiation dose that can be applied safely to cancer patients. In our study, collagen contents of the liver and ileum were significantly increased following irradiation, indicating enhanced tissue fibrotic activity, while RVT treatment attenuated the fibrotic activity by its antioxidant properties. In support of these findings, we have previously shown that 10 mg/kg dose of the antioxidant resveratrol had exerted hepato- and gastroprotection against oxidative injury and exerted antifibrotic action on the injured tissues [19,53]. The present study is the first to demonstrate the protective effect of RVT on radiation-induced oxidative damage of the hepatic and ileal tissues, as well as of the leukocytes. On the other hand, it was previously shown that RVT acts synergistically with ionizing radiation to inhibit tumour cell survival, implicating that RVT can act as a potential radiation sensitizer, without inducing or enhancing spontaneously occurring apoptotic death in normal hematopoietic progenitor cells [54]. Moreover, the natural antioxidant RVT inhibits carcinogenesis in animal models through the inhibition of tumour initiation and progression processes [55–58].

In conclusion, the most important and innovative conclusion of the present work is that RVT, by its antioxidant properties, protects the vulnerable organs against oxidative damage. These results suggest that supplementing cancer patients with adjuvant therapy of RVT may aid in the alleviation of the side-effects due to radiation-induced oxidative organ injuries.

References

[1] Vijayalaxmi, Reiter RJ, Tan DX, Herman TS, Thomas CR Jr. Melatonin as a radioprotective agent: a review. Int J Radiat Oncol Biol Phys 2004;59:639–653.

[2] Rubin P, Johnston CJ, Williams JP, McDonald S, Finkelstein JN. A perpetual cascade of cytokines postirradiation leads to pulmonary fibrosis. Int J Radiat Oncol Biol Phys 1995;33:99–109.

[3] Daly JM, Bertagnoli M, De Cosse JJ, Morton DL. Oncology. In: SI Schwartz, editor. Principles of surgery. New York: McGraw-Hill; 1999. p 335–345.

[4] Agrawal A, Chandra D, Kale RK. Radiation induced oxidative stress: II studies in liver as a distant organ of tumor bearing mice. Mol Cell Biochem 2001;224:9–17.

[5] Riley PA. Free radicals in biology: oxidative stress and the effects of ionizing radiation. Int J Radiat Oncol Biol 1994;65:27–33.

[6] Morgan WF, Day JP, Kaplan MI, McGhee EM, Limoli CL. Genomic instability induced by ionizing radiation. Radiat Res 1996;146:247–258.

[7] Sener G, Jahovic N, Tosun O, Atasoy BM, Yeğen BC. Melatonin ameliorates ionizing radiation-induced oxidative organ damage in rats. Life Sci 2003;74:563–672.

[8] Patt HM, Turee EB, Straube RL, Smith DE. Cysteine protection against x irradiation. Science 1949;110:213–214.

[9] Bacq ZM, Herve A, Lecomte J, Fischer P, Blavier J. Protection against x-rays by beta-mercaptoethylamine. Arch Int Physiol 1951;59:442–447.

[10] Schucter LM, Glick JH. The current status of WR-2721 (amifostine): a chemotherapy and radiotherapy protector. In: VT Devita, S Hellman, SA Rosenberg, editors. Biologic therapy of cancer updates. Philadelphia: Lippincott; 1993. p 1–10.

[11] Fremont L. Biological effects of resveratrol. Life Sci 2000;66:663–673.
[12] Aggarwal BB, Bhardwaj A, Aggarwal RS, Seeram NP, Shishoda S, Takada Y. Role of resveratrol in prevention and therapy of cancer: preclinical and clinical studies. Anticancer Res 2004;24:2783–2840.
[13] Wallerath T, Deckert G, Ternes T, Anderson H, Li H, Witte K, Forstermann U. Resveratrol, a polyphenolic phytoalexin present in red wine, enhances expression and activity of endothelial nitric oxide synthase. Circulation 2002;106: 1652–1658.
[14] Dong Z. Molecular mechanisms of the chemopreventive effect of resveratrol. Mutat Res 2003;523–524:145–150.
[15] Wu JM, Wang ZR, Hsich TC, Bruder JL, Zou JG, Huang YZ. Mechanism of cardioprotection by resveratrol, a phenolic antioxidant present in red wine. Int J Mol Med 2001;8:3–17.
[16] Gresele P, Pignatelli P, Guglielmini G, Carnevale R, Mezzasoma AM, Ghiselli A, Momi S, Violi F. Resveratrol, at concentrations attainable with moderate wine consumption, stimulates human platelet nitric oxide production. J Nutr 2008;138:1602–1608.
[17] Notas G, Nifli AP, Kampa M, Vercauteren J, Kouroumalis E, Castanas E. Resveratrol exerts its antiproliferative effect on HepG2 hepatocellular carcinoma cells, by inducing cell cycle arrest, and NOS activation. Biochim Biophys Acta 2006;1760:1657–1666.
[18] Sener G, Topaloğlu N, Sehirli AO, Ercan F, Gedik N. Resveratrol alleviates bleomycin-induced lung injury in rats. Pulm Pharmacol Ther 2007;20:642–649.
[19] Sehirli O, Tozan A, Omurtag GZ, Cetinel S, Contuk G, Gedik N, Sener G. Protective effect of resveratrol against naphthalene-induced oxidative stress in mice. Ecotoxicol Environ Saf 2008;71:301–308.
[20] Moss DW, Henderson AR, Kachmar JF. Enzymes. In: NW Tietz, editor. Fundamentals of clinical chemistry. Philadelphia, WB Saunders Company; 1987. p 372–373.
[21] Martinek RG. A rapid ultraviolent spectrophotomeetric lactic dehydrogenase assay. Clin Chim Acta 1972;40:91–99.
[22] Takei H, Araki A, Watanabe H, Ichinose A, Sendo F. Rapid killing of human neutrophils by the potent activator phorbol 12-myristate 13-acetate (PMA) accompanied by changes different from typical apoptosis or necrosis. J Leukoc Biol 1996;59:229–240.
[23] Davies GR, Simmonds NJ, Stevens TRJ, Grandison A, Blake DR, Rampton DS. Mucosal reactive oxygen metabolite production in duodenal ulcer disease. Gut 1992;33: 1467–1472.
[24] Ohara Y, Peterson TE, Harrison DG. Hypercholesterolemia increases endothelial superoxide anion production. J Clin Invest 1993;91:2546–2551.
[25] Haklar G, Yüksel M, Yalçın AS. Chemiluminescence in the measurement of free radicals: theory and application on a tissue injury model. Marmara Med J 1998;11:56–60.
[26] Beuge JA, Aust SD. Microsomal lipid peroxidation. Methods Enzymol 1978;53:302–311.
[27] Beutler E. Glutathione in red blood cell metabolism. A manual of biochemical methods. New York: Grune & Stratton; 1975. p 112–114.
[28] Hillegass LM, Griswold DE, Brickson B, Albrightson-Winslow C. Assessment of myeloperoxidase activity in whole rat kidney. J Pharmacol Methods 1990;24:285–295.
[29] Lopez De Leon A, Rojkind M. A simple micromethod for collagen and total protein determination in formalin-fixed parraffin-embedded sections. J Histochem Cytochem 1985;33:737–743.
[30] Wyllie H. Glucocorticoid induced thymocyte apoptosis is associated with endogenous endonuclease activation. Nature 1980;284:555–556.
[31] Burton K. A study of the conditions and mechanism of the diphenylamine reaction for the colorimetric estimation of deoxyribonucleic acid. Biochem J 1956;62:315–323.
[32] Reading HW, Isbir T. The role of cation activated ATPase in transmitter release from the rat iris. Q J Exp Physiol Cogn Med Sci 1980;65:105–116.
[33] Fiske CH, Subbarow Y. The colorimetric determination of phosphorus. J Biol Chem 1925;66:375–400.
[34] Lowry OH, Rosenbrough NJ, Farr AL, Randall RJ. Protein measurements with the folin phenol reagent. J Biol Chem 1951;193:265–275.
[35] Pandey BN, Lathika KM, Mishra KP. Modification of radiation-induced oxidative damage in liposomal and microsomal membrane by eugenol. Radiat Phys Chem 2006;75:384–391.
[36] Nair CK, Parida DK, Nomura T. Radioprotectors in radiotherapy. J Radiat Res 2001;42:21–37.
[37] Park K, Lee JH. Protective effects of resveratrol on UVB-irradiated HaCaT cells through attenuation of the caspase pathway. Oncol Rep 2008;19:413–417.
[38] Black HS. Reassessment of a free radical theory of cancer with emphasis on ultraviolet carcinogenesis. Integr Cancer Ther 2004;3:279–293.
[39] Saada HN, Said UZ, Meky NH, Abd El Azime AS. Grape seed extract Vitis vinifera protects against radiation-induced oxidative damage and metabolic disorders in rats. Phytother Res 2009;23:434–438.
[40] Yildiz OG, Soyuer S, Saraymen R, Eroglu C. Protective effects of caffeic acid phenethyl ester on radiation induced lung injury in rats. Clin Invest Med 2008;31:E242–E247.
[41] Lin JK, Tsai SH. Chemoprevention of cancer and cardiovascular disease by resveratrol. Proc Natl Sci Counc Repub China B 1999;23:99–106.
[42] Das S, Khan N, Mukherjee S, Bagchi D, Gurusamy N, Swartz H, Das DK. Redox regulation of resveratrol-mediated switching of death signal into survival signal. Free Radic Biol Med 2008;4:82–90.
[43] Sebai H, Ben-Attia M, Sani M, Aouani E, Ghanem-Boughanmi N. Protective effect of resveratrol on acute endotoxemia-induced nephrotoxicity in rat through nitric oxide independent mechanism. Free Radic Res 2008;42:913–920.
[44] Tatlidede E, Sehirli O, Velioğlu-Oğünc A, Cetinel S, Yeğen BC, Yarat A, Süleymanoğlu S, Sener G. Resveratrol treatment protects against doxorubicin-induced cardiotoxicity by alleviating oxidative damage. Free Radic Res 2009;43:195–205.
[45] Swantek JL, Tsen MF, Cobb MH, Thomas JA. IL-1 receptor associated kinase modulates host responsiveness to endotoxin. J Immunol 2000;164:4301–4306.
[46] Lin HI, Chu SJ, Wang D, Feng NH. Pharmacological modulation of TNF production in macrophages. J Microbiol Immunol Infect 2004;37:8–15.
[47] Sullivan GW, Sarembock IJ, Linden J. The role of inflammation in vascular diseases. J Leukoc Biol 2000;67:591–602.
[48] Kettle AJ, Winterbourn CC. Myeloperoxidase: a key regulator of neutrophil oxidant production. Redox Report 1997;3:3–15.
[49] Prabhu R, Balasubramanian KA. Effect of oxidants on small intestinal brush border membranes and colonic apical membranes—a comparative study. Comp Biochem Physiol C Toxicol Pharmacol 2003;134:329–339.
[50] Keelan M, Walker K, Cheeseman CI, Thomson AB. Two weeks of oral synthetic E2 prostaglandin (Enprostil) improves the intestinal morphological but not the absorptive response in the rat to abdominal irradiation. Digestion 1992;53: 101–107.
[51] Lebrun F, Benderitter M, Berroud A, Voisin P, Griffiths NM. Potential role of the membrane in the development of intestinal cellular damage after whole-body gamma irradiation of the rat. Can J Physiol Pharmacol 2002;80:686–693.

[52] Franklin TJ. Therapeutic approaches to organ fibrosis. Int J Biochem Cell Biol 1997;29:79–89.
[53] Solmaz A, Şener G, Çetinel S, Yüksel M, Yeğen C, Yeğen BC. Protective and therapeutic effects of resveratrol on acetic acid-induced gastric ulcer. Free Radic Res 2009;43:594–603.
[54] Scarlatti F, Sala G, Ricci C, Maioli C, Milani F, Minella M, Botturi M, Ghidoni R. Resveratrol sensitization of DU145 prostate cancer cells to ionizing radiation is associated to ceramide increase. Cancer Lett 2007;253:124–130.
[55] Jang M, Cai L, Udeani GO, Slowing KV, Thomas CF, Beecher CW, Fong HH, Farnsworth NR, Kinghorn AD, Mehta RG, Moon RC, Pezzuto JM. Cancer chemopreventive activity of resveratrol, a natural product derived from grapes. Science 1997;275:218–220.
[56] Bhat KP, Lantvit D, Christov K, Mehta RG, Moon RC, Pezzuto JM. Estrogenic and antiestrogenic properties of resveratrol in mammary tumor models. Cancer Res 2001;61:7456–7463.
[57] Li ZG, Hong T, Shimada Y, Komoto I, Kawabe A, Ding Y, Kaganoi J, Hashimoto Y, Imamura M. Suppression of N-nitrosomethylbenzylamine (NMBA)-induced esophageal tumorigenesis in F344 rats by resveratrol. Carcinogenesis 2002;23:1531–1536.
[58] Seve M, Chimienti F, Devergnas S, Aouffen M, Douki T, Chantegrel J, Cadet J, Favier A. Resveratrol enhances UVA-induced DNA damage in HaCaT human keratinocytes. Med Chem 2005;1:629–633.

This paper was first published online on iFirst on 21 August 2009.